

On the problem of generalizing the semiconductor Bloch equations from a closed to an open system

*Original*

On the problem of generalizing the semiconductor Bloch equations from a closed to an open system / PROIETTI ZACCARIA, R.; Rossi, Fausto. - In: PHYSICAL REVIEW. B, CONDENSED MATTER AND MATERIALS PHYSICS. - ISSN 1098-0121. - 67:11(2003), pp. 113311-1-113311-4. [10.1103/PhysRevB.67.113311]

*Availability:*

This version is available at: 11583/1405258 since: 2016-09-13T11:20:34Z

*Publisher:*

APS American Physical Society

*Published*

DOI:10.1103/PhysRevB.67.113311

*Terms of use:*

openAccess

This article is made available under terms and conditions as specified in the corresponding bibliographic description in the repository

*Publisher copyright*

(Article begins on next page)

# On the problem of generalizing the semiconductor Bloch equation from a closed to an open system

Remo Proietti Zaccaria\* and Fausto Rossi†

*Istituto Nazionale per la Fisica della Materia (INFM) and Dipartimento di Fisica, Politecnico di Torino, Corso Duca degli Abruzzi 24, 10129 Torino, Italy*

(Received 2 December 2002; published 19 March 2003)

A microscopic theory for the description of quantum-transport phenomena in systems with open boundaries is proposed. We shall show that the application of the conventional Wigner-function formalism to this problem leads to unphysical results, such as injection of coherent electronic states from the contacts. To overcome such basic limitation, we propose a generalization of the standard Wigner-function formulation, able to properly describe the incoherent nature of carrier injection at the device spatial boundaries as well as the interplay between phase coherence and energy relaxation/dephasing within the device active region. The proposed theoretical scheme constitutes a quantum-mechanical derivation of the phenomenological injection model commonly employed in the simulation of open quantum devices.

DOI: 10.1103/PhysRevB.67.113311

PACS number(s): 72.10.Bg, 85.30.-z, 73.40.-c

Present-day technology pushes device dimensions toward limits where the traditional semiclassical transport theory<sup>1</sup> can no longer be applied, and more rigorous quantum-transport approaches are required.<sup>2</sup> However, in spite of the quantum-mechanical nature of carrier dynamics in the core region of typical nanostructured devices—such as semiconductor superlattices and double-barrier structures—the overall behavior of such quantum systems is often the result of a complex interplay between phase coherence and energy relaxation/dephasing,<sup>3</sup> the latter being primarily due to the presence of spatial boundaries.<sup>4</sup> It follows that a proper treatment of the nanoscale devices requires a theoretical modeling able to properly account for both coherent—i.e., scattering-free—and incoherent—i.e., phase-breaking—processes on the same footing. To this end, a generalization to open systems—i.e., systems with open boundaries—of the well-known semiconductor Bloch equations<sup>5</sup> (SBE) has been recently proposed.<sup>6</sup> However, the theoretical analysis presented in Ref. 6 is primarily related to the interplay between phase coherence and energy relaxation within the device active region, and—apart from its abstract formulation—no detailed investigation of the carrier-injection process (from the electrical contacts into the device active region) has been performed so far.

Aim of the present paper is to provide a quantum-mechanical description of the coupling dynamics between the device active region and external charge reservoirs, able to account for the semiphenomenological injection models commonly employed in state-of-the-art simulations of realistic one- and two-dimensional open quantum devices.<sup>7</sup> Among such simulation strategies it is worth mentioning the approach recently proposed by Fischetti and co-workers.<sup>8</sup> By denoting with  $f_\alpha$  the carrier distribution over the electronic states  $\alpha$  of the device and with  $W_{\alpha\alpha'}$  the microscopic scattering rates (due, e.g., to carrier-carrier and carrier-phonon interaction), the transport equation proposed in Ref. 8 is of the form:<sup>9</sup>

$$\frac{d}{dt}f_\alpha = \sum_{\alpha'} (W_{\alpha\alpha'}f_{\alpha'} - W_{\alpha'\alpha}f_\alpha) + \frac{f_\alpha^b - f_\alpha}{\tau_\alpha}. \quad (1)$$

Here,  $f_\alpha^b$  denotes the equilibrium carrier distribution in the contacts, while  $\tau_\alpha$  can be regarded as the device transit time for an electron in state  $\alpha$ . As anticipated, in spite of a rigorous treatment of the scattering dynamics (via the standard Boltzmann collision term involving microscopic scattering rates<sup>1</sup>  $W_{\alpha\alpha'}$ ), the last (relaxation-time-like) term describes carrier injection/loss on a partially phenomenological level and does not depend on the real position of the device spatial boundaries. Indeed, although the transit time  $\tau$  is related to the device dimensions, the semiclassical distribution function  $f_\alpha$  does not provide a fully quantum-mechanical real-space description.

In order to provide a fully microscopic real-space formulation of the carrier-injection process, we shall start revisiting the theoretical approach proposed in Ref. 6. The starting point is the conventional SBE for a closed system:<sup>5,6,10</sup>

$$\frac{d}{dt}\rho_{\alpha_1\alpha_2} = \sum_{\alpha'_1\alpha'_2} L_{\alpha_1\alpha_2,\alpha'_1\alpha'_2}\rho_{\alpha'_1\alpha'_2}, \quad (2)$$

where the effective Liouville operator

$$L_{\alpha_1\alpha_2,\alpha'_1\alpha'_2} = \frac{1}{i\hbar}(\epsilon_{\alpha_1} - \epsilon_{\alpha_2})\delta_{\alpha_1\alpha_2,\alpha'_1\alpha'_2} + \Gamma_{\alpha_1\alpha_2,\alpha'_1\alpha'_2} \quad (3)$$

is the sum of two terms: coherent (i.e., scattering-free) single-particle evolution ( $\epsilon_\alpha$  denoting the single-particle energy of state  $\alpha$ ) plus energy-relaxation/-dephasing dynamics; the latter is described in terms of the scattering tensor  $\Gamma$ , whose explicit form, given in Ref. 5, involves the microscopic in- and out-scattering rates for the various interaction mechanisms considered. The key idea proposed in Ref. 6 is to apply the usual Weyl-Wigner transform

$$u_{\alpha_1\alpha_2}(\mathbf{r},\mathbf{k}) = \int d\mathbf{r}' \phi_{\alpha_1}\left(\mathbf{r} + \frac{\mathbf{r}'}{2}\right) \frac{e^{-i\mathbf{k}\cdot\mathbf{r}'}}{(2\pi)^{3/2}} \phi_{\alpha_2}^*\left(\mathbf{r} - \frac{\mathbf{r}'}{2}\right), \quad (4)$$

[ $\phi_\alpha(\mathbf{r}) \equiv \langle \mathbf{r} | \alpha \rangle$  denoting the single-particle wave function of state  $\alpha$ ] to the SBE in Eq. (2). In this way the latter is

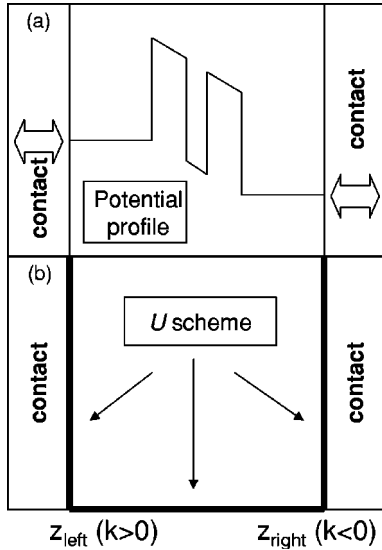


FIG. 1. Schematic representation of the device active region sandwiched between its electrical contacts (a) and of the corresponding  $U$  boundary-condition scheme for a one-dimensional system. The latter implies, in particular, the knowledge of the incoming Wigner function  $f(z_b, k)$ , i.e.,  $f(z_{\text{left}}, k > 0)$  and  $f(z_{\text{right}}, k < 0)$ .

translated into its phase-space representation  $\mathbf{r}, \mathbf{k}$ , which allows to impose to the Wigner function<sup>4</sup>

$$f(\mathbf{r}, \mathbf{k}) = \sum_{\alpha_1 \alpha_2} u_{\alpha_1 \alpha_2}(\mathbf{r}, \mathbf{k}) \rho_{\alpha_1 \alpha_2}, \quad (5)$$

the desired values at the device spatial boundaries according to the well-known “ $U$  scheme” depicted in Fig. 1. More specifically, in order to impose the desired spatial boundary conditions to the equation of motion for  $f$ , we add and subtract a source term

$$S(\mathbf{r}, \mathbf{k}) = v(\mathbf{k}) f^b(\mathbf{k}) \delta(\mathbf{r} - \mathbf{r}_b), \quad (6)$$

where  $v(\mathbf{k})$  denotes the negative or incoming part of the carrier group velocity normal to the boundary surface and  $f^b(\mathbf{k})$  is the Wigner function describing the distribution of the injected carriers. By applying the inverse of the Weyl-Wigner transform in Eq. (4) to the new equation of motion for  $f$ , we finally get

$$\frac{d}{dt} \rho_{\alpha_1 \alpha_2} = \sum_{\alpha'_1 \alpha'_2} \tilde{L}_{\alpha_1 \alpha_2, \alpha'_1 \alpha'_2} \rho_{\alpha'_1 \alpha'_2} + S_{\alpha_1 \alpha_2}, \quad (7)$$

where the effective Liouville operator  $\tilde{L}$  corresponds to the operator  $L$  in Eq. (3) renormalized by

$$\Delta L_{\alpha_1 \alpha_2, \alpha'_1 \alpha'_2} = - \int d\mathbf{r}_b d\mathbf{k} u_{\alpha_1 \alpha_2}^*(\mathbf{r}_b, \mathbf{k}) v(\mathbf{k}) u_{\alpha'_1 \alpha'_2}(\mathbf{r}_b, \mathbf{k}) \quad (8)$$

and  $S_{\alpha_1 \alpha_2}$  is the Weyl-Wigner antitransform of the source term in Eq. (6). Equation (7) is the desired generalization to open systems of the SBE in Eq. (2).<sup>11</sup>

In order to validate the theoretical approach presented so far, we shall focus on a very simple semiconductor nano-

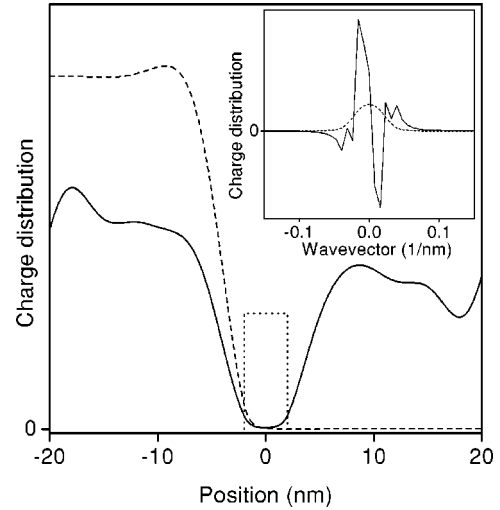


FIG. 2. Comparison between the real-space charge distribution obtained from the phenomenological injection model in Eq. (1) [ $n(\mathbf{r}) = \sum_{\alpha} f_{\alpha} |\phi_{\alpha}(\mathbf{r})|^2$ —dashed curve] and the microscopic model in Eq. (9) [ $n(\mathbf{r}) = \sum_{\alpha_1 \alpha_2} \rho_{\alpha_1 \alpha_2} \phi_{\alpha_1}(\mathbf{r}) \phi_{\alpha_2}^*(\mathbf{r})$ —solid curve] for a GaAs-based single-barrier structure (height  $V_0 = 0.5$  eV and width  $a = 4$  nm) equidistant from the electrical contacts. In this room-temperature simulation, due to a misalignment  $\Delta\mu = 0.2$  eV of the left and right chemical potential, carriers are primarily injected from left (total carrier concentration  $n \approx 10^{17} \text{ cm}^{-3}$ ). The corresponding charge distribution in momentum space is also reported in the inset (see text).

structure: a single-barrier equidistant from the device contacts (see Fig. 2). As basis states  $\alpha$ , we adopt the scattering states of the device potential profile; moreover, to better identify the role played by carrier injection, we shall neglect all other sources of energy relaxation/dephasing in the device active region, like carrier-phonon and carrier-carrier scattering:  $\Gamma_{\alpha_1 \alpha_2, \alpha'_1 \alpha'_2} = 0$  [see Eq. (3)]. Under these assumptions, Eq. (7) in steady-state conditions reduces to

$$\frac{i}{\hbar} (\epsilon_{\alpha_1} - \epsilon_{\alpha_2}) \rho_{\alpha_1 \alpha_2} - \sum_{\alpha'_1 \alpha'_2} \Delta L_{\alpha_1 \alpha_2, \alpha'_1 \alpha'_2} \rho_{\alpha'_1 \alpha'_2} = S_{\alpha_1 \alpha_2}. \quad (9)$$

Figure 2 shows results for the single-barrier potential profile when carriers are primarily injected from left. Here, the simulated real-space charge distribution obtained from the phenomenological injection model in Eq. (1) (dashed curve) is compared to that of the microscopic model in Eq. (9) (solid curves). As we can see, the two models give completely different results. The phenomenological model gives basically what we expect: since we have significant carrier injection from left only and since the potential barrier is relatively high, the carrier distribution is mainly located on the left side. In contrast, the microscopic model gives an almost symmetric charge distribution. In order to understand the origin of this unphysical result, let us focus on the nature of the source term in Eq. (7). Contrary to the phenomenological injection/loss term in Eq. (1), the latter is intrinsically non-diagonal, i.e., the injection of a carrier with well-defined wave vector  $\mathbf{k}$  [see Eq. (6)] is described by a nondiagonal

source contribution  $S_{\alpha_1\alpha_2}$ . In other words, *we inject into the device active region a coherent superposition of states  $\alpha_1$  and  $\alpha_2$* , in clear contrast with the idea of injection from a thermal—i.e., diagonal—charge reservoir. More specifically, in this case the generic scattering state  $\alpha$  on the left comes out to be an almost equally weighted superposition of  $+k$  and  $-k$ :  $\phi_k(z) = a_k e^{ikz} + b_k e^{-ikz}$ . This, in turn, tells us that the generic plane-wave state  $k$  injected from the left contact is also an almost equally weighted superposition of the left and right scattering states. This is why the charge distribution (solid curve in Fig. 2) is almost symmetric: any electron injected from left couples to left as well as to right scattering states. The anomaly of the microscopic model is even more pronounced if we look at the carrier distribution in momentum space (see inset in Fig. 2). While for the phenomenological model (dashed curve), we get a positive-definite distribution showing, as expected, the two symmetric wave-vector components of the scattering state, the microscopic result is not positive definite; this tells us that the boundary-condition scheme considered so far does not provide a “good” Wigner function.

The scenario previously discussed is highly nonphysical; it can be mainly ascribed to the boundary-condition scheme employed so far, which implies injection of plane-wave electrons [see source term in Eq. (6)], regardless of the shape of the device potential profile. This is an intrinsic limitation of the conventional Wigner-function representation  $\mathbf{r}, \mathbf{k}$ . It is then clear that, in order to overcome this limitation, what we need is *a boundary-condition scheme realizing diagonal injection over the scattering states  $\alpha$  of the device potential profile*.

To this end, in this paper, we propose a generalization of the Wigner-function formulation considered so far. The key idea is to extend the Weyl-Wigner transform in Eq. (4) from the  $\mathbf{k}$  to a generic basis set  $\{|\beta\rangle\}$  according to<sup>12</sup>

$$\bar{u}_{\beta_1\beta_2}^{\alpha_1\alpha_2}(\mathbf{r}) = \Omega \int d\mathbf{r}' \phi_{\alpha_1}\left(\mathbf{r} + \frac{\mathbf{r}'}{2}\right) \chi_{\beta_1}^*\left(\mathbf{r} + \frac{\mathbf{r}'}{2}\right) \times \chi_{\beta_2}\left(\mathbf{r} - \frac{\mathbf{r}'}{2}\right) \phi_{\alpha_2}^*\left(\mathbf{r} - \frac{\mathbf{r}'}{2}\right), \quad (10)$$

where  $\Omega$  denotes the volume of the simulated region. In analogy to Eq. (5), our generalized Wigner function is given by<sup>13</sup>

$$\bar{f}_{\beta_1\beta_2}(\mathbf{r}) = \sum_{\alpha_1\alpha_2} \bar{u}_{\beta_1\beta_2}^{\alpha_1\alpha_2}(\mathbf{r}) \rho_{\alpha_1\alpha_2}. \quad (11)$$

By combining Eqs. (5) and (11), the new Wigner function  $\bar{f}$  can be easily expressed in terms of the standard one as

$$\bar{f}_{\beta_1\beta_2}(\mathbf{r}) = \int d\mathbf{r}' d\mathbf{k}' \mathcal{K}_{\beta_1\beta_2}(\mathbf{r}; \mathbf{r}', \mathbf{k}') f(\mathbf{r}', \mathbf{k}'), \quad (12)$$

with

$$\mathcal{K}_{\beta_1\beta_2}(\mathbf{r}; \mathbf{r}', \mathbf{k}') = \sum_{\alpha_1\alpha_2} \bar{u}_{\beta_1\beta_2}^{\alpha_1\alpha_2}(\mathbf{r}) u_{\alpha_1\alpha_2}^*(\mathbf{r}', \mathbf{k}'). \quad (13)$$

The new Wigner function can then be regarded as a sort of convolution of the original one with the kernel  $\mathcal{K}$  in Eq. (13). This may recall a well-established procedure used to obtain positive-definite phase-space quantum distributions, the so-called “smoothing procedure.”<sup>14</sup> However, we stress that this is not the case: (i) here there is no need for a positive-definite function, and (ii) contrary to the standard smoothing procedure, the initial and final phase spaces do not coincide ( $\mathbf{r}', \mathbf{k}' \rightarrow \mathbf{r}, \beta_1\beta_2$ ).

By adopting as basis states  $|\beta\rangle$  again the scattering states of the device potential profile  $|\alpha\rangle$ , and assuming a diagonal source term of the form

$$\bar{S}_{\alpha_1\alpha_2}(\mathbf{r}) = v_{\alpha_1} f_{\alpha_1}^b \delta_{\alpha_1\alpha_2} \delta(\mathbf{r} - \mathbf{r}_b), \quad (14)$$

the equation of motion for the new Wigner function  $\bar{f}$  in Eq. (11) will be given by

$$\frac{d}{dt} \bar{f}_{\alpha_1\alpha_2}(\mathbf{r}) = \sum_{\alpha'_1\alpha'_2} \int d\mathbf{r}' \tilde{L}_{\alpha_1\alpha_2, \alpha'_1\alpha'_2}(\mathbf{r}, \mathbf{r}') \bar{f}_{\alpha'_1\alpha'_2}(\mathbf{r}') + \bar{S}_{\alpha_1\alpha_2}(\mathbf{r}), \quad (15)$$

with a renormalization  $\Delta L_{\alpha_1\alpha_2, \alpha'_1\alpha'_2}(\mathbf{r}, \mathbf{r}')$  given by

$$-v_{\alpha_1} \delta_{\alpha_1, \alpha_2} \delta_{\alpha_1\alpha_2, \alpha'_1\alpha'_2} \delta(\mathbf{r} - \mathbf{r}_b) \delta(\mathbf{r} - \mathbf{r}'). \quad (16)$$

We stress that now the source term  $\bar{S}$  in Eq. (14) describes diagonal injection over the scattering states (with velocity  $v_\beta$ ), as requested. Indeed, if we now integrate Eq. (15) over the real-space coordinate  $\mathbf{r}$ , we get again the density-matrix equation in Eq. (7), but now with a diagonal source term  $S_{\alpha_1\alpha_2} = v_{\alpha_1} f_{\alpha_1}^b \delta_{\alpha_1\alpha_2}$  and a much simpler—i.e., partially diagonal—renormalization term  $\Delta L_{\alpha_1\alpha_2, \alpha'_1\alpha'_2} = -v_{\alpha_1} \delta_{\alpha_1\alpha_2} \bar{u}_{\alpha'_1\alpha'_2}^{\alpha_1\alpha_2}(\mathbf{r}_b)$ . In the scattering-free case, the stationary solution is again described by Eq. (9). However, due to the diagonal nature of the new source term as well as of the partially diagonal structure of  $\Delta L$ , Eq. (9) has now a diagonal solution:  $\rho_{\alpha_1\alpha_2} = f_{\alpha_1} \delta_{\alpha_1\alpha_2}$ . More specifically, the diagonal density-matrix elements  $f_\alpha$  obey the following steady-state equation:

$$\sum_{\alpha'} \mathcal{T}_{\alpha\alpha'} f_{\alpha'} = f_\alpha^b, \quad (17)$$

with  $\mathcal{T}_{\alpha\alpha'} = \bar{u}_{\alpha'\alpha'}^{\alpha\alpha}(\mathbf{r}_b)$ . Equation (17) is semiclassical in nature, i.e., it involves diagonal density-matrix terms only. However, contrary to the phenomenological injection model in Eq. (1), here the distribution function in state  $\alpha$  is the result of an “incoherent superposition” from all the injection channels:  $f_\alpha = \sum_{\alpha'} \mathcal{T}_{\alpha\alpha'}^{-1} f_{\alpha'}^b$ . We finally stress that, by replacing the  $\mathcal{T}$  with the identity operator ( $\mathcal{T}_{\alpha\alpha'} = \delta_{\alpha\alpha'}$ ), the phenomenological injection model in Eq. (1) is recovered. Figure 3 shows again results for the single-barrier potential profile previously considered. Here, the simulation based on the phenomenological injection model in Eq. (1) (dashed curves) is compared to that of the new microscopic model in

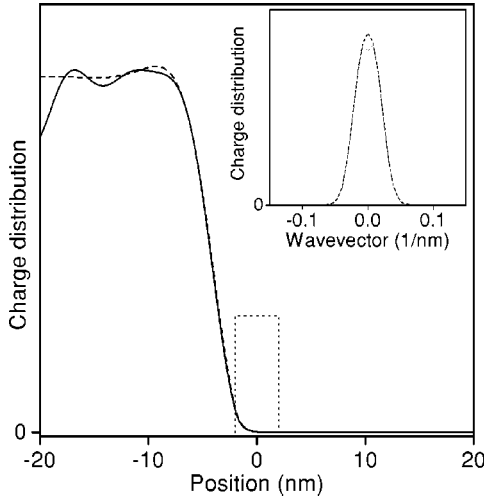


FIG. 3. Same as in Fig. 2 but for the new microscopic model in Eq. (17) (see text).

Eq. (17) (solid curves). As we can see, the highly nonphysical behaviors of Fig. 2 (solid curves) have been completely removed. Indeed, the momentum distribution in the inset is always positive-definite and the two models exhibit a very similar behavior. We find relatively small deviations close to the device spatial boundaries, which can be ascribed to the interlevel injection coupling  $T_{\alpha\alpha'}$ , [see Eq. (17)], not present in the phenomenological injection model. This is clearly a fingerprint of our real-space description, where the pointlike carrier injection is located at the device spatial boundaries. However, when the device active region is relatively far from the contacts these deviations can be safely neglected, and the

phenomenological model in Eq. (1) provides reliable results.

At this point, a question needs to be answered: *Would it be possible to describe the diagonal injection over the scattering states in Eq. (14) by means of a “ad hoc” source term  $S(\mathbf{r}, \mathbf{k})$  within the standard phase space?* The answer to this question is yes. However, a closer inspection reveals that such an “ad hoc” function can never be pointlike in space, which in turn does not allow to employ the conventional boundary-condition approach considered so far (see Fig. 1), where we impose the value of the Wigner distribution only at the device spatial boundaries by means of an effective pointlike source term [see Eq. (14)]. Therefore, the generalized Weyl-Wigner representation proposed in this paper is not only physically sound, but it allows to maintain all the well-known advantages of the standard boundary condition scheme. We finally stress that the analysis proposed is not “self-consistent,” i.e., there is no self-consistent solution of Schrödinger and Poisson equations; however, the latter can be implemented exactly as in the standard Wigner-function approach.

In conclusion, we have proposed a quantum treatment of transport phenomena in systems with open boundaries. Our analysis has shown that the conventional Wigner-function formalism leads to unphysical results, such as injection of coherent superpositions of states from the device spatial boundaries. This basic limitation has been removed by introducing a generalization of the standard Wigner-function formulation, able to properly describe the incoherent nature of carrier injection. The proposed theoretical scheme constitutes a rigorous derivation of the phenomenological injection models commonly employed in the simulation of open quantum devices.

\*Email address: Proietti@Athena.PoliTo.It

†Email address: FRossi@Athena.PoliTo.It

<sup>1</sup>See, e.g., C. Jacoboni and P. Lugli, *The Monte Carlo Method for Semiconductor Device Simulations* (Springer, Wien, 1989).

<sup>2</sup>See, e.g., in *Theory of Transport Properties of Semiconductor Nanostructures*, edited by E. Schöll (Chapman and Hall, London, 1998).

<sup>3</sup>See, e.g., R.C. Iotti and F. Rossi, Phys. Rev. Lett. **87**, 146603 (2001).

<sup>4</sup>See, e.g., W. Frensley, Rev. Mod. Phys. **62**, 745 (1990), and references therein.

<sup>5</sup>See, e.g., F. Rossi and T. Kuhn, Rev. Mod. Phys. **74**, 895 (2002), and references therein.

<sup>6</sup>F. Rossi, A. Di Carlo, and P. Lugli, Phys. Rev. Lett. **80**, 3348 (1998).

<sup>7</sup>See, e.g., in *Computational Electronics*, special issue of VLSI design **13**, 1 (2001).

<sup>8</sup>M.V. Fischetti, Phys. Rev. B **59**, 4901 (1999).

<sup>9</sup>See Eqs. (41) and (42) in Ref. 8.

<sup>10</sup>Here,  $\rho_{\alpha_1\alpha_2}$  is the single-particle density matrix written in our single-particle basis  $\{|\alpha\rangle\}$ . Its diagonal elements correspond to the usual distribution function  $f_\alpha$  of the semiclassical theory

(Ref. 1), while the off-diagonal terms ( $\alpha_1 \neq \alpha_2$ ) describe the degree of quantum-mechanical phase coherence between states  $\alpha_1$  and  $\alpha_2$ .

<sup>11</sup>The open character of the system results in a non-Hermitian correction  $\Delta L$  to the Liouville operator  $L$ , whose effect is equivalent to a purely dissipative process within the simulated region, as originally pointed out in Ref. 4.

<sup>12</sup>Here, the set of basis functions  $\chi_\beta(\mathbf{r}) \equiv \langle \mathbf{r} | \beta \rangle$  is, in general, different from the basis set  $\phi_\alpha$ . It is easy to show that if we consider as basis states  $|\beta\rangle$  conventional plane waves, the standard Weyl-Wigner transform in Eq. (4) is recovered. We stress that—contrary to Eq. (4)—this new Weyl-Wigner transform is not a unitary transformation corresponding to a simple basis change; it amounts to a nontrivial projection operation involving the real-space Wigner coordinate  $\mathbf{r}$ :  $\bar{u}_{\beta_1\beta_2}^{\alpha_1\alpha_2}(\mathbf{r}) = \langle \beta_1 | \alpha_1 \rangle \langle \mathbf{r} | \langle \alpha_2 | \beta_2 \rangle$ .

<sup>13</sup>In analogy to the conventional Wigner-function theory (Ref. 4), the real-space charge distribution (see solid line in Fig. 3) is now given by  $n(\mathbf{r}) = \sum_{\beta} \bar{f}_{\beta}(\mathbf{r})$ .

<sup>14</sup>See, e.g., P. Bertrand *et al.*, Phys. Lett. **94A**, 415 (1983), and references therein.